Numerical Investigation of Rail Longitudinal Vibration Mode on Corrugation Formation

Zhang, Pan; Li, Zili

DOI
10.1007/978-3-031-66971-2_114

Publication date
2024

Document Version
Final published version

Published in
Advances in Dynamics of Vehicles on Roads and Tracks III

Numerical Investigation of Rail Longitudinal Vibration Mode on Corrugation Formation

Pan Zhang(✉) and Zili Li

Section of Railway Engineering, Delft University of Technology, Stevinweg 1, 2628 CN Delft, The Netherlands
p.zhang@tudelft.nl

Abstract. Short pitch corrugation is a typical defect on rail surfaces that induces high level of noise and increases maintenance costs. Despite numerous research efforts, corrugation development mechanism has not yet been fully understood and root-cause solutions have not been developed. This work numerally simulates the rail corrugation in the V-Track test rig, aiming to better understand corrugation mechanism and also link the scaled laboratory tests to the full-scale reality. A three-dimensional finite element model of the V-Track is established to simulate the vehicle-track dynamic interaction. The fastening and ballast parameters are calibrated by fitting the simulated track receptances to hammer tests. Rail corrugation with a major wavelength of 5.7 mm is successfully reproduced using the FE model, which shares features similar to the experimentally produced corrugation in the V-Track. The numerical simulation demonstrates that a rail longitudinal compression mode at 790 Hz is the 'wavelength-fixing' mechanism of corrugation in the V-Track, agreeing with the experimental results. This work numerically verifies the dominance of the rail longitudinal vibration modes on corrugation formation.

Keywords: Short pitch corrugation · rail longitudinal vibration mode · initial excitation · V-Track test rig · 3D vehicle-track dynamic model

1 Introduction

Short pitch corrugation (hereinafter corrugation) is recognized as the (quasi-) periodic undulation of rail surfaces on straight tracks or gentle curves with a typical wavelength range of 20–80 mm [1], see an example in Fig. 1. Rail corrugation excites large wheel-rail impact force, causes excessive vibration and noise, and accelerates the deterioration of the track components (e.g., fastenings, sleepers and ballast), which considerably increases maintenance costs. Furthermore, corrugation may also induce rolling contact fatigue (RCF) cracks (e.g., squats [2]) that threaten the train operation safety. Therefore, it is of great significance to understand the corrugation formation mechanism and develop effective mitigation methods.

Numerous theoretical and experimental studies of corrugation have been conducted in the past decades as summarized in the review papers [1, 3]. The corrugation formation process is generally considered a feedback loop that consists of a 'wavelength-fixing' mechanism and a damage mechanism [1]. The 'wavelength-fixing mechanism

W. Huang and M. Ahmadian (Eds.): IAVSD 2023, LNME, pp. 1108–1117, 2025.
https://doi.org/10.1007/978-3-031-66971-2_114

Fig. 1. Short pitch Corrugation observed in the Dutch railway with a wavelength of approximately 30 mm.

is essentially frequency-selection in resonance [4]. While the damage mechanism is commonly assumed as differential wear, the 'wavelength-fixing' mechanism has not yet been completely clear. Among the many hypotheses, the vertical pinned-pinned resonance has been widely attributed to a wavelength-fixing mechanism supported by numerical simulations and measurements [5–7]. However, there are difficulties to explain some field observations about corrugation with the pinned-pinned resonance. First, corrugation occurs only at some places but pinned-pinned resonance is everywhere in the discretely-supported tracks. Second, the single pinned-pinned resonance cannot explain the relatively small variation of wavelength with large variation in vehicle speed. Third, Corrugation has been observed on embedded rail systems where pinned-pinned resonance is absent. Therefore, more research endeavours are still needed to fully understand the corrugation phenomenon.

Recently, new insight has been gained in [4] into the corrugation formation mechanism employing an advanced 3D finite element (FE) vehicle-track interaction model. Corrugation initiation and consistent growth have been successfully reproduced that share features similar to field corrugation. It is found that rail longitudinal compression modes, instead of the commonly considered vertical modes, are responsible for corrugation initiation with the necessary initial excitation that allows flexibility for longitudinal vibration. To validate this hypothesis, an experimental study of corrugation has been performed using a downscale V-Track test rig [8]. Compared to other testing facilities, the V-Track has better dynamic similarity to the real vehicle-track system [9]. Corrugation with a wavelength of 6.0 mm has been successfully produced on the rail surface.

To link the scaled laboratory tests to the full-scale reality, numerical simulation of the corrugation in the V-Track is needed with the same modelling approach as in [4]. With this link, findings from the tests of corrugation development and anti-corrugation measures in the V-Track can be quickly transferred to the real-life railway system.

This paper aims to develop a numerical model that can reproduce the corrugation in the V-Track, with emphasis on the verification of the dominance of rail longitudinal vibration modes on corrugation formation. The structure of this work is as follows. Section 2 introduces the corrugation experiments in the V-Track and the 3D FE model of

the vehicle-track dynamic interaction. Section 3 calibrates the track parameters including the fastening and ballast stiffness and damping using the hammer tests. Section 4 presents the numerical reproduction of corrugation and analyze its formation mechanism. The main conclusions are drawn in Sect. 5.

2 Methodology

In this section, the corrugation experiment and the 3D FE model of the V-Track are introduced.

2.1 The V-Track Test Rig and Corrugation Experiments

The V-Track test rig consists of two wheel assemblies (W1 and W3 in short) running over a ring track system, see Fig. 2. The wheel assemblies are fixed on the steel frames, which are together pulled by a 'driving motor' to run on the ring track. Another 'braking motor' is also used to apply a controllable torque on the wheels to generate braking /traction forces. The two wheels are cylindrical with a radius of 65 mm and they were cutting from the real wheel rim to ensure identical materials. The ring track system consists of four sections of rails connecting through rail joints. They were also cut from the real rail heads and have the same rail profile with a head curvature radius of 60 mm. Important track components that influence the wheel-track dynamic interaction, such as fastenings, sleepers and ballast elasticity are included in the track system and their parameters are designed according to the similarity law [9]. The loads of the V-Track in the vertical, longitudinal and lateral directions are controllable by adjusting the suspension preloads, wheel torque and angle of attack (AoA), respectively. Therefore, the wheel-rail dynamic interaction on both the tangent and curved tracks can be simulated using the V-Track.

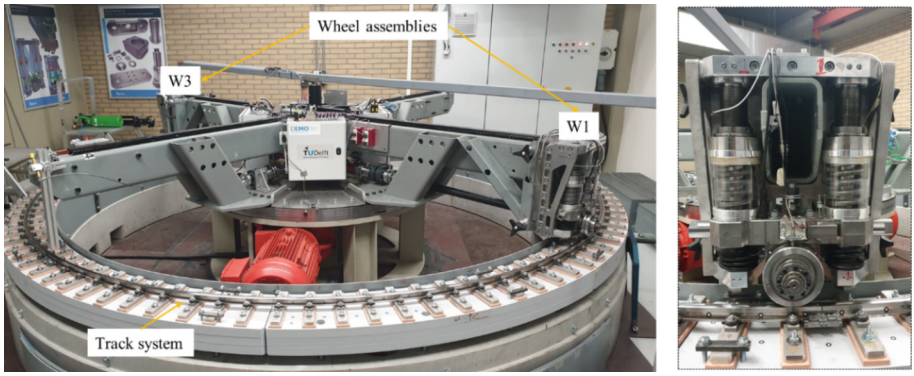

Fig. 2. The V-Track test rig for corrugation experiments [8].

In the corrugation experiment, the vertical (normal) loads on both wheels were around 4 kN, resulting in a maximum contact pressure of 1.35 Gpa. The AoA of both wheels was designed to be as small as possible to simulate the wheel-rail lateral interaction

on a tangent track. The braking motor was used to adjust one wheel torque (W1) that achieved an adhesion coefficient of around 0.1 and the other (W3) as small as possible, to simulate the driving and driven wheels, respectively. The wheel running speed was 16 km/h. Fastening clips were completely loosened for every other sleeper to simulate the degraded fastenings on the rails of R220 and R260MN. 3D HandyScan tests were performed to measure the corrugation geometry. Hammer tests were performed to obtain the dynamic behaviours of the track and the wheels, which are related to the corrugation characteristic frequency and wavelength. The contact forces are acquired with a sampling frequency of 16.67 kHz using a dynamometer, which consists of four 3-component piezoelectric force sensors mounted between the wheel assembly and the steel frame [8].

Corrugation was successfully produced on the rail R220 with a major wavelength (l) component of 6.0 mm, as shown in Fig. 3a and b. With a speed (v) of 16 km/h, the characteristic frequency (f) of the corrugation in the V-Track is 741 Hz, calculated by $f = v/l$. By comprehensively analyzing the measured corrugation geometry, wheel-rail contact forces and track dynamics, it is found that the rail longitudinal vibration mode at 750 Hz and its induced longitudinal dynamic force are the 'wavelength-fixing' mechanism of rail corrugation in the V-Track test rig, as shown in Fig. 3c and d.

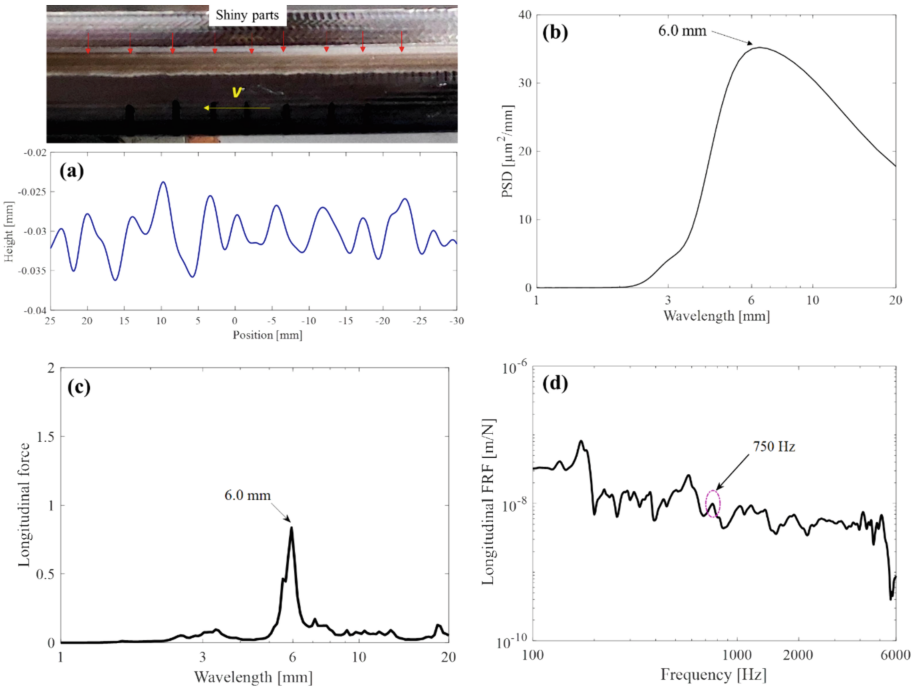

Fig. 3. Experimental results of rail corrugation in the V-Track. (a) Produced rail corrugation on R220 and its geometry in the spatial domain; (b) corrugation with a major wavelength component at 6.0 mm; (3) longitudinal dynamic force dominates corrugation formation at 6.0 mm; (d) the rail longitudinal vibration mode at 750 Hz is the 'wavelength-fixing' mechanism of corrugation.

2.2 3D FE Model of the V-Track

A 3D FE vehicle-track interaction model of the V-Track is developed, as shown in Fig. 4. The axes X, Y, and Z refers to the longitudinal (rolling), lateral and vertical directions, respectively. The wheel, rail and sleepers were modeled using 8-node solid elements based on their real geometries and materials. Nonuniform meshing is employed to achieve computation efficiency, and the finest meshing size in the solution zone is 0.2 mm to ensure calculation accuracy for the wheel-rail rolling contact. The primary suspension, fastenings and ballast were modeled by spring-damper elements. The wheel-rail contact model applied an automatic surface-to-surface contact scheme based on the penalty contact algorithm. The wheel-rail friction coefficient was 0.35 [10]. An implicit-explicit sequential approach was employed in the simulation to minimize the solution time and the dynamic effects during the initialization of wheel-rail interaction. In the explicit calculation, the initial translation velocity of 4.44 m/s (16 km/h) and rotation velocity of 68.31 rad/s are prescribed to the wheel. An initial compression displacement is set to suspension springs to apply a wheel preload of 4 kN. A braking torque of 23 N.m and a zero AoA is applied to the wheel to adjust the wheel-rail friction force. The adopted integration time step was sufficiently small (15 ns) to ensure the stability of the integration and the contact. The fastening parameters play an important role in corrugation formation. Experimental results indicate that the loose fastening clamps serve as an effective initiation excitation in corrugation initiation [8]. To simulate the loose fastenings, smaller stiffness and damping are applied in the fastening model and their values are quantitatively derived by fitting the simulated frequency response functions (FRFs) to the measured ones from hammer tests. They are listed in Table 1 together with the ballast parameters and the nominal material properties of the wheel, the rail and the sleeper.

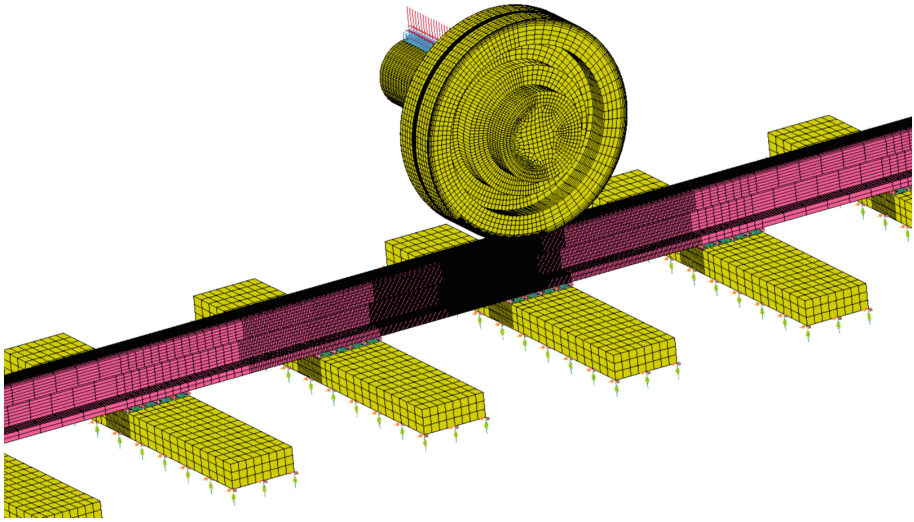

Fig. 4. 3D FE vehicle-track dynamic model of the V-Track.

Table 1. Values of parameters in the 3D FE vehicle-track model of the V-Track.

Components	Parameter	Value
Wheel, rail, sleeper	Young's modulus	210 GPa
	Poisson's ratio	0.3
	Density	7850 kg/m^3
Suspension	Vertical stiffness	230 kN/m
	Vertical damping	100 N.s/m
Fastening	Vertical stiffness	85 MN/m
	Vertical damping	2.5 kN.s/m
	Longitudinal stiffness	10 MN/m
	Longitudinal damping	4.8 kN.s/m
	Lateral stiffness	10 MN/m
	Lateral damping	4.8 kN.s/m
Rubber pad (ballast)	Vertical stiffness	15 MN/m
	Vertical damping	250 N.s/m
	Longitudinal stiffness	1.2 MN/m
	Longitudinal damping	175 N.s/m
	Lateral stiffness	1.2 MN/m
	Lateral damping	200 N.s/m

2.3 Wear Model

The damage by wear Wf at a point in the rail surface is assumed to be proportional to the accumulated frictional work done during wheel passages [11]. When such a point is represented by a surface element, the frictional work is calculated for each wheel passage, i.e., from the element entering until leaving the contact patch, as follows:

$$W_f(\mathrm{x}, \mathrm{y}) = \mathrm{k} w_f(\mathrm{x}, \mathrm{y}) = \mathrm{k} \sum\nolimits_{\mathrm{i}=1}^{N} \tau_i(\mathrm{x}, \mathrm{y}) v_i(\mathrm{x}, \mathrm{y}) \cdot \mathrm{t} \tag{1}$$

where k is the wear coefficient, wf (x, y) is the frictional work, τi (x, y) and vi (x, y) are the local tangential stress and slip, respectively, and N is the number of time steps Δt during which the element passes through the contact patch.

3 Track Parameter Calibration

The track parameters, including the stiffness and damping of the fastenings and rubber pads, are calibrated by fitting the simulated receptances to the measured ones from hammer tests. Figure 5 shows the closest fit of the simulation to the measurement in the vertical direction. It can be seen that the overall tendency and amplitude of the simulation match the measurement well up to 6 kHz. Further, the simulation result successfully

reproduces the four major characteristic frequencies at about 360 Hz, 1100 Hz, 2600 Hz and 4600 Hz. The modal analysis results indicate that they correspond to the full track resonance mode, sleeper bending modes, rail resonance and pinned-pinned resonance modes, respectively. Good agreement has also been achieved between the simulated and measured track receptances in the longitudinal and lateral directions, indicating the accuracy of the FE model and in reproducing 3D track dynamics.

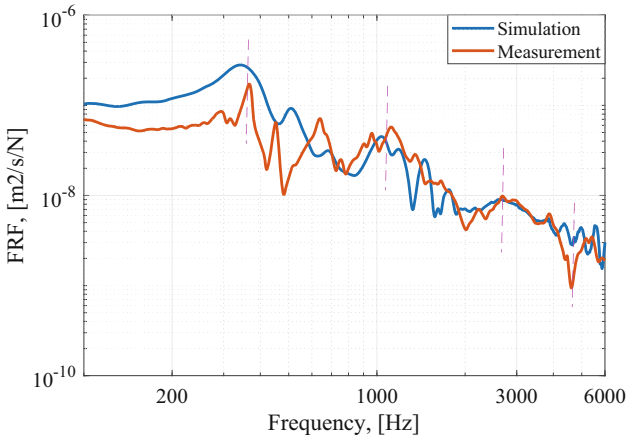

Fig. 5. Comparison between simulated and measured track receptances in the vertical direction.

4 Corrugation Reproduction and Formation Mechanism

When the wheel rolls over the rail with loose fastenings, wheel-rail dynamic forces are induced, causing differential wear and corrugation formation on the rail surface. Figure 6 shows the simulated initial differential wear from the 3D FE model in the spatial and wavelength domains. These results are normalized and bandpass filtered between 2 mm and 15 mm. It can be seen from Fig. 6a that the initial differential wear has large fluctuation amplitude and will cause corrugation after multiple wheel passages. The major wavelength component is at about 5.7 mm, as shown in Fig. 6b. Comparing Fig. 6 with the experimentally produced corrugation in Fig. 3a and 3b, it can be seen that the simulated differential wear is similar to the measured corrugation geometry in terms of the spatial distribution and the dominant wavelength component. This agreement indicates that the 3D FE model can successfully reproduce the rail corrugation in the V-Track.

Meanwhile, it is observed that the simulated differential wear does not include the long-wavelength components (e.g., 8 mm–15 mm) that exist in the measured corrugation geometry in Fig. 3b. The possible reason is that in the FE simulation, the rail surface is smooth without considering the initial surface roughness that exists in reality. Besides, the lateral wheel-rail dynamic interaction is underestimated in the FE simulation with a zero AoA, which shows relatively strong fluctuation in the V-Track tests. The lateral dynamic force in the experiments may contribute to the development of this long-wavelength roughness.

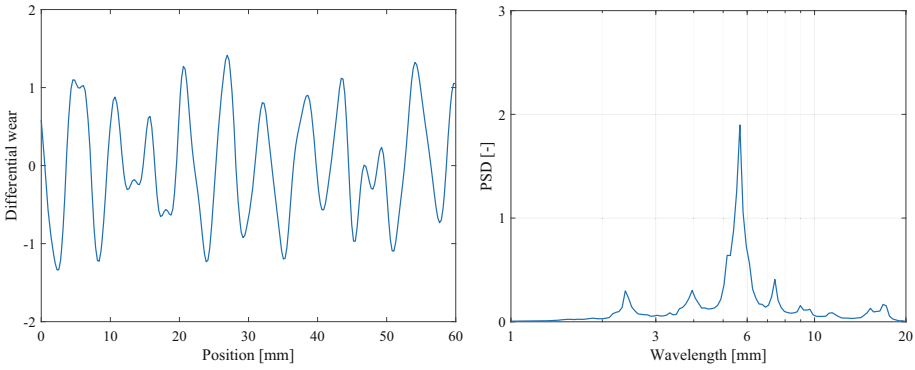

Fig. 6. The simulated initial differential wear from the 3D FE model. (a) In the spatial domain; (b) in the wavelength domain.

In order to further study the 'wavelength-fixing' mechanism of corrugation, a modal analysis was performed using the FE model with loose fastenings. A rail longitudinal compression mode at about 790 Hz is identified that corelates well to the simulated corrugation frequency of about 780 Hz, as shown in Fig. 7. This mode frequency is slightly higher than the experimental corrugation frequency of about 740 Hz, which may be related to the fastening model and parameters and will be further investigated in future research. The numerical simulations are consistent with the experimental evidences that indicate rail longitudinal vibration model and its induced longitudinal dynamic force dominates corrugation formation in the V-Track. Furthermore, the finding about the dominance of rail compression mode on corrugation formation in this work agrees with the full-scale 3D FE simulation of field corrugation [4].

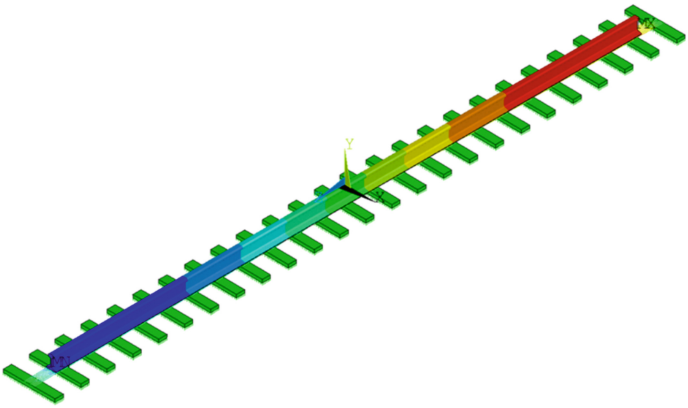

Fig. 7. Rail longitudinal compression mode at 790 Hz.

5 Conclusions

In this work, numerical simulation of the corrugation in the V-Track is performed to better understand corrugation mechanism and link the scaled laboratory tests to the full-scale reality. Through this link, findings from the tests of corrugation formation and mitigation measures in the V-Track can be more conveniently transferred to the real-life railway system. First, the structure of the V-Track and the corrugation experiment are briefly introduced. Corrugation was produced on the rail surface. Experimental evidences indicate that rail longitudinal vibration model and its induced longitudinal dynamic force are dominant for corrugation formation with the initial excitation from loose fastenings.

Afterwards, a 3D FE vehicle-track dynamic model of the V-Track is established. The parameters of the fastening model are calibrated by fitting the simulated track receptances to hammer tests. Corrugation is successfully reproduced using the FE mode with a major wavelength component of 5.7 mm, and it share features similar to the experimentally produced corrugation in the V-track in the spatial and wavelength domains. The modal analysis results demonstrate that a rail longitudinal compression mode at 790 Hz is 'wavelength-fixing' mechanism of the corrugation in the V-Track, matching well with the experimental results.

In summary, this work verifies the dominance of rail longitudinal vibration mode on corrugation formation and contributes to a better understanding of corrugation formation mechanism. In future work, the fastening models and parameters will be further investigated to gain insights for corrugation mitigation approaches.

References

1. Grassie, S., Kalousek, J.: Rail corrugation: characteristics, causes and treatments. Proc. Inst. Mech. Eng., Part F: J. Rail Rapid Transit **207**, 57–68 (1993)
2. Deng, X., Qian, Z., Li, Z., Dollevoet, R.: Investigation of the formation of corrugation-induced rail squats based on extensive field monitoring. Int. J. Fatigue **112**, 94–105 (2018)
3. Oostermeijer, K.: Review on short pitch rail corrugation studies. Wear **265**, 1231–1237 (2008)

4. Li, Z., Li, S., Zhang, P., Núñez, A., Dollevoet, R.: Mechanism of short pitch rail corrugation: initial excitation and frequency selection for consistent initiation and growth. Int. J. Rail Transport. **12**, 1–36 (2022)
5. Hempelmann, K., Knothe, K.: An extended linear model for the prediction of short pitch corrugation. Wear **191**, 161–169 (1996)
6. Hiensch, M., Nielsen, J.C., Verheijen, E.: Rail corrugation in The Netherlands—measurements and simulations. Wear **253**, 140–149 (2002)
7. Nielsen, J.: Numerical prediction of rail roughness growth on tangent railway tracks. J. Sound Vib. **267**, 537–548 (2003)
8. Zhang, P., Li, Z.: Experimental study of short pitch corrugation using a vehicle-track interaction test RIG (2022)
9. Naeimi, M., Li, Z., Petrov, R.H., Sietsma, J., Dollevoet, R.: Development of a new downscale setup for wheel-rail contact experiments under impact loading conditions. Exp. Tech. **42**, 1–17 (2018)
10. Yang, Z., Zhang, P., Moraal, J., Li, Z.: An experimental study on the effects of friction modifiers on wheel–rail dynamic interactions with various angles of attack. Railw. Eng. Sci. **30**, 360–382 (2022)
11. Neilsen, J.: Evolution of rail corrugation predicted with a non-linear wear model. J. Sound Vib. **227**, 915–933 (1999)